Numerical simulation of the twist-grain-boundary phase of chiral liquid crystals

doi: 10.1103/PhysRevE.73.060701

PHYSICAL REVIEW E **73**, 060701(R) (2006)

Numerical simulation of the twist-grain-boundary phase of chiral liquid crystals

Hiroto Ogawa* and Nariya Uchida
Department of Physics, Tohoku University, Sendai, 980-8578, Japan
(Received 8 March 2006; published 19 June 2006)

We study the structure of the twist-grain-boundary phase of chiral liquid crystals by numerically minimizing the Landau–de Gennes free energy. We analyze the morphology of layers at the grain boundary, to better understand the mechanism of frustration between the smectic layer order and chirality. As the chirality increases, the layer compression energy strongly increases while the effective layer bending rigidity is reduced due to unlocking of the layer orientation and the director. This results in large deviation of the layer morphology from that of Scherk's first minimal surface and linear stack of screw dislocations.

DOI: 10.1103/PhysRevE.73.060701 PACS number(s): 61.30.Jf, 61.72.Mm, 61.20.Ja

Frustration causes complex structural patterns in a variety of materials and over different length scales. To resolve the frustration, the equilibrium patterns often contain topological defects. Liquid crystals are some of the richest materials providing a variety of frustrated defect phases. Defects are inevitably formed by frustration between the smectic order and chirality, because the periodic layer structure and continuous helical structure are geometrically incompatible. As a result, the frustration gives rise to a set of screw dislocations. The simplest stable phase containing such defects is the twist-grain-boundary (TGB) phase, the existence of which was predicted using the analogy with the Abrikosov vortex lattice of type-II superconductors [1]. In this phase, smectic slabs of a certain length (grains) are twisted by a certain angle from their neighbors and separated from them by a narrow region (grain boundary) in which screw dislocations are aligned.

After its theoretical prediction [1] and experimental confirmation [2], study of the TGB phase was extended to other chiral frustrated phases and transitions between them. Theoretically, thermal fluctuation changes the transitions between smectic-*A* (Sm-*A*), TGB_A, TGB_C, and cholesteric (N^*) phases from second to first order. In parallel to the vortex liquid phase of superconductors, fluctuation induces the melted TGB phase or the chiral line phase (N_{L^*}) with a melted defect lattice, which was theoretically predicted [3] and experimentally confirmed [4,5]. Many other chiral frustrated phases have been found and reported [6,7].

On the other hand, the spatial structure of the TGB phase, especially that of a grain boundary, still has much to be understood. Kamien and Lubensky [8] showed that the grain boundary structure is well described by a linear stack of screw dislocations (LSD) if the twist angle α is close to zero. For small α, the layer structure is also approximated by Scherk's first minimal surface. However, the minimal surface defined by vanishing mean curvature H is achieved when the bending elasticity is the only contribution to the free energy. Deviation from the minimal surface should occur due to the other elastic effects, namely, the layer compression and the twist Frank energies. Also, spatial variation of the density near the TGB defect core is not considered in the previous analytic studies, and the interplay between these effects remains to be investigated [9–11]. Study of the TGB structure for large twist angles should also be helpful for understanding the structure of more complex phases, such as the NL^* and smectic blue phases [6,12].

It might be worth mentioning that the TGB structure is also exhibited by other materials such as twisted lamellae of block copolymer melts [13] and defect-containing Turing patterns in a reaction-diffusion system [14]. The mechanism that determines the defect structure depends on the material, and the uniqueness of the liquid crystal TGB structure is not yet clarified.

In this Rapid Communication, we study the core structure of a grain boundary by numerical minimization of the Landau–de Gennes free energy. Thus, compared to previous molecular simulations of the TGB phase [15,16], our results allow more direct comparison with analytical results. Also, the previous simulations suffer from severe finite-size effects because the size of the simulation box and the grain size ℓ_b are generally incommensurate with each other. By focusing on a single grain boundary, we become free from this problem and can study the core structure with a higher resolution. The neglected grain boundary interaction would not affect the core structure except in the vicinity of the TGB-N^* transition. The difference between the simulation result and the model surfaces (i.e., Scherk's first surface and the LSD) is analyzed as a function of the twist angle α. We discuss the reason for the deviation in terms of the coupling between the smectic order parameter and the director.

The free energy we utilize is the covariant Landau–de Gennes model expressed as [1,17]

$$F = F_{DW} + F_{int} + F_{Frank}, \tag{1}$$

$$F_{DW} = \int d\boldsymbol{r} \frac{g}{4}\left(\frac{\tau}{g} + |\Psi|^2\right)^2, \tag{2}$$

$$F_{int} = \int d\boldsymbol{r} \frac{B}{2}|(\boldsymbol{\nabla} - iq_0\boldsymbol{n})\Psi|^2, \tag{3}$$

*Electronic address: hiroto@cmpt.phys.tohoku.ac.jp

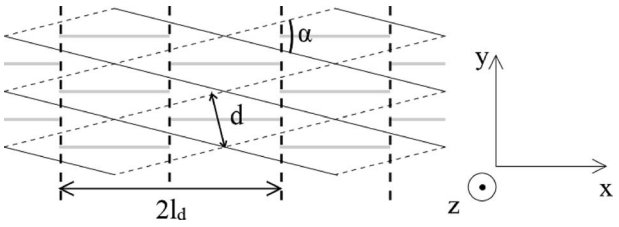

FIG. 1. Single twist-grain-boundary structure. The broken and gray lines indicate the parallel screw dislocations and the smectic layers in the grain boundary plane ($z=0$). The solid and dotted lines are the layers at $z\to\pm\infty$, respectively.

$$F_{Frank}=\int d\boldsymbol{r}\left(\frac{K_1}{2}(\boldsymbol{\nabla}\cdot\boldsymbol{n})^2+\frac{K_2}{2}(\boldsymbol{n}\cdot\boldsymbol{\nabla}\times\boldsymbol{n}-k_0)^2+\frac{K_3}{2}(\boldsymbol{n}\times\boldsymbol{\nabla}\times\boldsymbol{n})^2\right), \tag{4}$$

where Ψ is the smectic (complex) order parameter combining the density modulation ($\propto \mathrm{Re}\Psi$) and layer displacement, and $\boldsymbol{n}$ is the director. The double-well potential F_{DW} with the dimensionless temperature τ controls the order-disorder (TGB-N^* or Sm-A-N^*) transition. The interaction part F_{int} with the coupling constant B fixes the layer thickness d to $2\pi/q_0$. The third term is the Frank elastic energy. Although the ratios between the Frank elastic constants K_i affect the dislocation core structure [18], we set all the Frank constants to the same value K and focus on the role of chirality and coupling between Ψ and $\boldsymbol{n}$. The correlation length of the order parameter Ψ is defined as $\xi=\sqrt{B/|\tau|}$, the director penetration length $\lambda=\sqrt{Kg/B|\tau|}$ and the Ginzburg parameter $\kappa\equiv\lambda/\xi=\sqrt{gK}/q_0B$. The TGB phase is stable only when $\kappa>1/\sqrt{2}$ according to the mean-field theory [1].

The numerical minimization is performed in an $L_x\times L_y\times L_z$ simulation box, with the y and z axes identified with the direction of dislocations and the helical axis, respectively. To fix the transverse dimensions L_x and L_y, we fix the twist angle per grain boundary α as an independent parameter, instead of the chirality k_0. Then, two smectic slabs sandwiching a single grain boundary satisfy a two-dimensional (2D) crystalline symmetry with the periods $\ell_x=d/\sin(\alpha/2)$ and $\ell_y=d/\cos(\alpha/2)$ (see Fig. 1). Thus we can assume the periodic boundary condition in the transverse directions. We set $L_x=\ell_x$ and $L_y=\ell_y$ to save computation time. The layer orientation changes by the angle α along the helical axis, which is imposed as a boundary condition at $z=0$ and $z=L_z$ as follows. The director is set to $\boldsymbol{n}=\boldsymbol{n}_\pm=(\pm\sin(\alpha/2),\cos(\alpha/2),0)$ at $z=L_z$ and $z=0$, respectively, while the smectic order parameters at these boundaries are connected by inversion with respect to the plane $x=L_x/2$: $\Psi(x,y,0)=\Psi(L_x-x,y,L_z)$. The latter is compatible with the 2D crystalline symmetry in the xy plane. For finite L_z, these boundary conditions induce interaction of the grain boundary and its images. However, the interaction is expected to decay exponentially [1] and hence our boundary condition gives a good approximation if $L_z/2\geqslant\xi,\lambda$. We will use $L_z=2d$ in the simulation.

The free energy is minimized by solving the time-dependent Ginzburg-Landau equations,

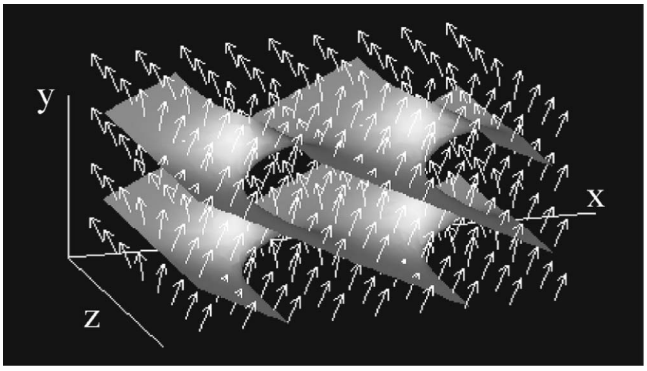

FIG. 2. Snapshot of the grain boundary structure at $\tau=-0.02$, $g=1$, $B=0.2$, $K=0.02$, and $\alpha=50°$. Plotted are the isosurface $\mathrm{Re}\Psi=0$ and the director $\boldsymbol{n}$ (arrows).

$$\frac{\partial\Psi}{\partial t}=-\Gamma_\Psi\frac{\delta F}{\delta\Psi}, \tag{5}$$

$$\frac{\partial\boldsymbol{n}}{\partial t}=-\Gamma_n(\mathbf{1}-\boldsymbol{nn})\cdot\frac{\delta F}{\delta\boldsymbol{n}}, \tag{6}$$

where Γ_Ψ and Γ_n are appropriate kinetic constants and the factor $1-nn$ in Eq. (6) ensures that $|n|^2=1$. For the initial condition we take two flat smectic slabs with sinusoidal order parameter profiles and layer normals identical to $\boldsymbol{n}_\pm$ for $z>L_z/2$ and $z<L_z/2$ (respectively). Since we fixed α instead of k_0, the chirality is determined by minimizing F_{Frank} with respect to k_0 as

$$k_0=\frac{1}{V}\int d\boldsymbol{r}(\boldsymbol{n}\cdot\boldsymbol{\nabla}\times\boldsymbol{n}), \tag{7}$$

which is calculated from the director configuration. In equilibrium, it is a function of the temperature τ and the twist angle α: $k_0=f(\tau,\alpha)$. Inverting this relation, we can find the equilibrium twist angle for given temperature and chirality as $\alpha=g(\tau,k_0)$. We use the parameter set $\tau=-0.02$, $g=1$, $B=0.2$, $K=0.02$, and $d=16$ with the unit mesh size $\Delta x=1$, unless otherwise stated. For this choice, the correlation length and the penetration length are $\xi=0.44d$ and $\lambda=0.80d$ so that the conditions $L_z/2\geqslant\xi,\lambda$ and $\kappa>1/\sqrt{2}$ are satisfied. The kinetic coefficients are chosen as $\Gamma_\psi=\Gamma_n=0.1$ with the time step $\Delta t=1$. Our criterion of equilibration is that the free energy difference $F_i(t+t_0)-F_i(t)$ is lower than 0.01% of the characteristic amount of $F_i\ \forall\ i$, where the index i indicates each free energy component and the relaxation time t_0 is determined by the fitting $F(t)\sim\exp(-t/t_0)+\mathrm{const}$ at the early stage $t\leqslant 2000$. To prevent a trapping by local free energy minima, we also added a small noise which is gradually reduced to zero. The equilibrated grain boundary structure for $\alpha=50°$ is shown in Fig. 2.

We first compare the obtained layer structure with Scherk's first surface. The deviation from the minimal surface can be estimated using the spatial average of H^2:

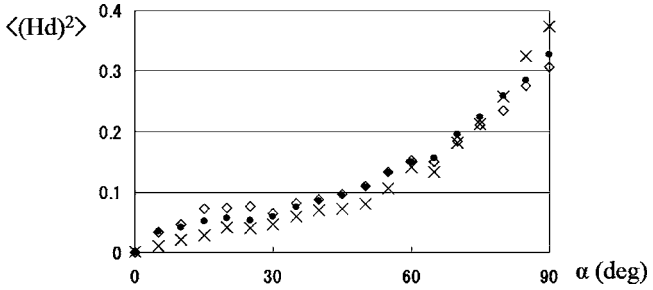

FIG. 3. The spatial average of the squared and dimensionless mean curvature $\langle (Hd)^2 \rangle$ versus the twist angle α at $\tau=(\times)$ −0.005, $(\diamond)$ −0.02, and $(\bullet)$ −0.05.

$$\langle H^2 \rangle = \frac{1}{V} \int d\boldsymbol{r}\, H^2 \tag{8}$$

This measure has more direct physical meaning than the previous ones [13] because Eq. (8) is proportional to the bending elastic energy of layers. The mean curvature is calculated through the layer normal $\boldsymbol{m}$ as $H=\boldsymbol{\nabla}\cdot\boldsymbol{m}$, while $\boldsymbol{m}$ is calculated through the phase Φ of the smectic order parameter Ψ as $\boldsymbol{m}=\boldsymbol{\nabla}\Phi/|\boldsymbol{\nabla}\Phi|$. In this way we can compute the mean curvature at every point, which is very important for averaging out the effect of mesh size.

The twist-angle dependence of the layer curvature is shown in Fig. 3. For small α, the TGB layer is close to Scherk's first surface, agreeing with the analytical calculation [8]. However, $\langle H^2 \rangle$ grows roughly linearly as a function of α. For large α, the mean curvature is not small even compared to the inverse layer thickness $1/d$.

To understand the origin of the deviation, we note that the layer bending elasticity has a contribution from Frank elasticity, through the coupling between Ψ and $\boldsymbol{n}$. To see this, it would be instructive to rewrite the interaction term F_{int} in the form

$$F_{int} = \frac{B}{2} \int d\boldsymbol{r} \left| i\,\boldsymbol{\nabla}\,|\Psi| - |\Psi||\boldsymbol{\nabla}\Phi|(\boldsymbol{m}-\boldsymbol{n}) - |\Psi|(|\boldsymbol{\nabla}\Phi| - q_0)\boldsymbol{n} \right|^2. \tag{9}$$

The first term homogenizes the order parameter amplitude, the second term locks the layer normal $\boldsymbol{m}$ and the director $\boldsymbol{n}$, and the third term is the layer compression term that adjusts the layer thickness. Thus the coupling between Ψ and $\boldsymbol{n}$ is divided into the locking and layer compression terms. If the locking effect is dominant, $\boldsymbol{m}$ and $\boldsymbol{n}$ will be identical. Then the splay term in the Frank elastic energy is converted into the layer bending energy, as $(K/2)\int d\boldsymbol{r}(\boldsymbol{\nabla}\cdot\boldsymbol{n})^2 = (K/2)\int d\boldsymbol{r}\, H^2$. However, if the locking is weak compared to the twist free energy $(\propto k_0)$ and/or the layer compression energy, an unlocking of $\boldsymbol{m}$ and $\boldsymbol{n}$ should occur. Then the splay term contributes less to the effective layer bending energy and $\langle H^2 \rangle$ can easily deviate from zero.

As α increases, the factor $(|\boldsymbol{\nabla}\Phi| - q_0)^2$ in the layer compression energy greatly increases [Fig. 4(b)], as it is approximated as $q_0^2\{\cos(\alpha/2)-1\}^2$ at the grain boundary core. Thus the frustration between layer compression and locking terms

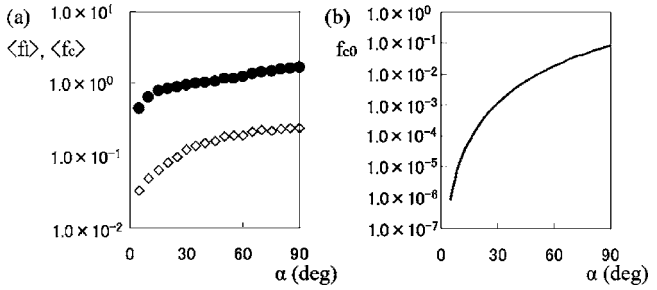

FIG. 4. (a) Twist-angle dependence of $(\bullet)$ the dimensionless locking energy $f_l=(g/|\tau|)\{|\Psi||\nabla\Phi|(m-n)d\}^2$ and $(\diamond)$ the dimensionless layer compression energy $f_c=(g/|\tau|)\{|\Psi_0|(|\nabla\Phi|-q_0)d\}^2$. (b) The layer compression factor $f_{c0}=\{\cos(\alpha/2)-1\}^2$ (see text).

increases and leads to the unlocking of $\boldsymbol{m}$ and $\boldsymbol{n}$. The spatially averaged angle between them is over $\simeq 20°$ for the standard parameter set and $\alpha=90°$. Note that the amplitude $|\Psi|$ near the grain boundary decreases as α increases at higher temperature, as shown in Fig. 5. However, it does not affect the ratio between the two free energy contributions and hence is not a major cause of the deviation from the minimal surface.

We further tested the role of director in two ways: (i) by decoupling the director from Ψ by turning off the Frank elasticity, and (ii) by adding an extra locking term $D(\boldsymbol{m}-\boldsymbol{n})^2$ to the free energy. In the unlocking limit (i), $\langle H^2 \rangle$ increased about five times, which proves Frank elasticity to be the major contribution to the layer bending rigidity. With (ii), $\langle H^2 \rangle$ is reduced to one-half for a weak extra locking [which reduces $\langle (\boldsymbol{m}-\boldsymbol{n})^2 \rangle$ by only 12%]. These results confirm that the director unlocking plays an important role in the deviation from the minimal surface.

Next we look at the temperature dependence. While we varied the temperature τ (roughly proportional to $\langle |\Psi|^2 \rangle$) by a factor of ten, the deviation $\langle H^2 \rangle$ showed only a small change. This also supports that the deviation is controlled mainly by the ratio between the above two free energy contributions. At

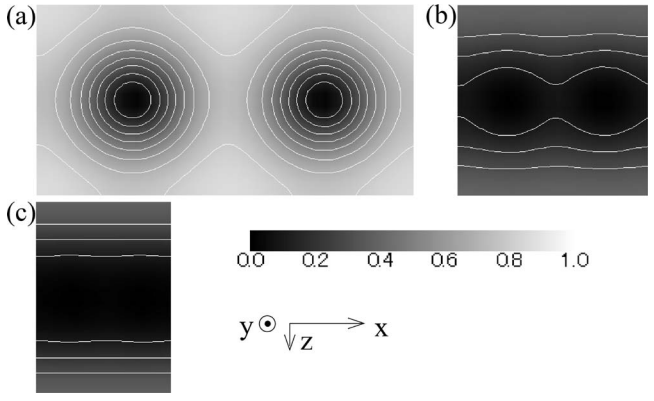

FIG. 5. The squared and dimensionless order parameter $|\Psi|^2/(|\tau|/g)$ in the cross section $y=$const at $\tau=-0.005$ and $\alpha=$(a) 30°, (b) 60°, and (c) 90°. The contour lines are drawn at 0.1, 0.2,…, 1.0. For large α, a significant melting of the smectic order is observed even far from the dislocation cores, while it is not seen at lower temperature.

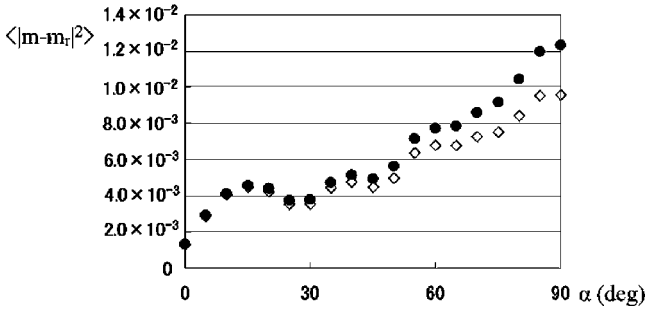

FIG. 6. Deviation of the layer normal from that of (●) Scherk's first surface and (◇) LSD. Each data set is smoothed by averaging over three consecutive points.

high temperature, the twist free energy becomes important compared to the locking term, which is reduced due to the prefactor $|\Psi|$. The deviation for a large twist angle is larger for higher temperature. This can be explained by the melting of the smectic order in the grain boundary, not only near the center of the dislocation core (Fig. 5).

Next, we compare the obtained layer structure with both Scherk's first surface and the LSD. To this end, we use the measure $\langle|\boldsymbol{m}-\boldsymbol{m}_r|^2\rangle$, where $\boldsymbol{m}_r=\nabla\Phi_r/|\nabla\Phi_r|$ is the normal vector of the reference surface defined by the phase function [10]

$$\Phi_r = \tan^{-1}\left[\tan\left(x\sin\frac{\alpha}{2}\right)\tanh\tilde{z}\right] + y\cos\frac{\alpha}{2} - \frac{\pi}{2}, \quad (10)$$

where $\tilde{z}=(z\sin\alpha)/2$ for Scherk's first surface and $\tilde{z}=z\sin(\alpha/2)$ for the LSD. The resultant deviations $\langle|\boldsymbol{m}-\boldsymbol{m}_{Scherk}|^2\rangle$ and $\langle|\boldsymbol{m}-\boldsymbol{m}_{LSD}|^2\rangle$ are plotted in Fig. 6. We see that the LSD gives a better approximation of the TGB structure for a large twist angle, while the difference is negligible for small α.

Finally let us compare our results with the TGB structure in twisted layers of block copolymer melts [13]. In block copolymer melts, deviation of the intermaterial dividing the surface from the minimal surface is caused by the packing frustration [19], which corresponds to the layer compression energy of liquid crystals. A self-consistent field-theoretic calculation [13] shows that the LSD is a better model than Scherk's first surface, as in our case. However, the measure of deviation in [13] has the dimension of the squared layer displacement, which causes an apparent rise of the deviation as $\alpha\to 0$. To compare with our results, their measure must be multiplied by the square of the characteristic wave number, proportional to $\sin^2(\alpha/2)\sim\alpha^2$. Then the deviation from the LSD and minimal surfaces should converge to 0 as $\alpha\to 0$.

In summary, we have investigated the structure of a single grain boundary in the TGB phase. Sizable deviations from the model surfaces are obtained and interpreted by increase of the layer compression energy and unlocking of the director and the layer normal. At higher temperature and large twist angle, the smectic order melts even far from the dislocation core. We hope that the core structure may be observed experimentally, using the same kind of technique as used in the study of defect cores in the smectic phase [20]. We plan to simulate the N_{L^*} phase in the future, for which the weakening of effective layer bending elasticity may have some significant effect.

We are grateful to Toshihiro Kawakatsu, Helmut Brand, Jun-ichi Fukuda, and Tomonari Dotera for various helpful comments and discussions.

[1] S. R. Renn and T. C. Lubensky, Phys. Rev. A **38**, 2132 (1988).
[2] J. W. Goodby, M. A. Waugh, S. M. Stein, E. Chin, R. Pindak, and J. S. Patel, Nature (London) **337**, 449 (1989).
[3] R. D. Kamien and T. C. Lubensky, J. Phys. I **3**, 2131 (1993).
[4] T. Chan, C. W. Garland, and H. T. Nguyen, Phys. Rev. E **52**, 5000 (1995).
[5] L. Navailles, B. Pansu, L. Gorre-Talini, and H. T. Nguyen, Phys. Rev. Lett. **81**, 4168 (1998).
[6] *Chirality in Liquid Crystals*, edited by H. S. Kitzerow and C. Bahr (Springer-Verlag, New York, 2002).
[7] J. Yamamoto, I. Nishiyama, M. Inoue, and H. Yokoyama, Nature (London) **437**, 525 (2005).
[8] R. D. Kamien and T. C. Lubensky, Phys. Rev. Lett. **82**, 2892 (1999).
[9] I. Bluestein, R. D. Kamien, and T. C. Lubensky, Phys. Rev. E **63**, 061702 (2001).
[10] I. Bluestein and R. D. Kamien, Europhys. Lett. **59**, 68 (2002).
[11] C. D. Santangelo and R. D. Kamien, Phys. Rev. Lett. **96**, 137801 (2006).
[12] B. A. DiDonna and R. D. Kamien, Phys. Rev. Lett. **89**, 215504 (2002).
[13] D. Duque and M. Schick, J. Chem. Phys. **113**, 5525 (2000).
[14] A. D. Wit, P. Borckmans, and G. Dewel, Proc. Natl. Acad. Sci. U.S.A. **94**, 12765 (1997).
[15] R. Memmer, J. Chem. Phys. **114**, 8210 (2001).
[16] M. P. Allen, M. A. Warren, and M. R. Wilson, Phys. Rev. E **57**, 5585 (1998).
[17] P. G. de Gennes, *The Physics of Liquid Crystals* (Oxford University Press, London, 1974).
[18] S. Kralj and T. J. Sluckin, Phys. Rev. E **48**, R3244 (1993).
[19] M. W. Matsen and F. S. Bates, Macromolecules **29**, 7641 (1996).
[20] J. P. Michel, E. Lacaze, M. Goldmann, M. Gailhanou, M. de Boissieu, and M. Alba, Phys. Rev. Lett. **96**, 027803 (2006).